Ferroelectricity in Achiral Liquid-Crystal Systems**

By *Serguei V. Yablonskii*, *Eduardo A. Soto-Bustamante*,* *Rafael O. Vergara-Toloza*, and *Wolfgang Haase*

Ferroelectric and antiferroelectric properties are among the most spectacular manifestations of cooperative phenomena in condensed materials. These effects are observed in a wide diversity of materials, such as solids, composite ceramics, polymers, and liquid crystals. The most studied systems correspond to perovskites as inorganic materials, and chiral liquid crystals as organic materials.

This work shows that ferroelectricity can also be detected in systems consisting of liquid-crystalline monomer–polymer mixtures possessing no chiral centers at all—herein we present the first reported material of this nature.

Chiral liquid-crystalline systems are very interesting, since their ferro- or antiferroelectric properties can be controlled structurally. The usually applied routine approach for preparing such materials is essentially based on the use of chiral liquid-crystalline substances possessing a tilted smectic phase. In such cases, spontaneous polarization arises as a secondary order parameter.[1–3]

In 1996, we spearheaded the discovery of the first achiral, macroscopically polar liquid-crystalline system, consisting of an achiral side chain polymer and its monomer.[4] The clear-cut antiferroelectric order was first demonstrated by us in non-chiral tilted smectics, where the local polarization is in the tilt plane.[5,6] Of particular interest is the fact that neither of the two components, by themselves, manifested this behavior. The mixtures show antiferroelectric polarization hysteresis curves in the smectic C phase and, after undergoing a poling process by cooling to the glassy state, revealed high pyroelectric responses—of potential interest for applications such as IR or piezo-detectors.[4]

Almost at the same time, novel schemes were developed to successfully introduce antiferroelectric or ferroelectric properties into liquid-crystalline material systems without chiral centers. Bent-shaped molecules exhibit a different smectic-like ordering, with in-plane spontaneous polarization.[7] A previous successful scheme for designing achiral ferroelectric liquid crystals exploiting the so-called polyphylic effect was first realized by Tournilhac et al.[8]

In this communication, we give the first report on new, achiral ferroelectric polymer—homologous-monomer mixtures. In accordance with our previous work,[5,6] the same nomenclature is used: PM*n*R*m* where P denotes the backbone polymer; M*n* is a methacrylate group with *n* methylene units as the aliphatic spacer; R*m* is a rigid resorcylphenylimine group core (R) possessing an alkoxy flying tail with *m* methylene units located in the *para* position and bonded to M*n*.

The composites consist of the side chain polymer PM6R12 and different monomers, such as M4R5, M4R6, and M4R8 (homologs of the M6R12 monomer), mixed in a 2:1 molar ratio. The aim of this work was to study the influence of the different monomers on the pyroelectric response for the PM6R12–M4R5, PM6R12–M4R6, and PM6R12–M4R8 composites. The molecular-length variation of the monomer with respect to the polymer side chain creates the possibility of the monomer locating in different configurations between the mesogenic side chains of the polymer.

The chemical structure of M4R8 is shown in Scheme 1. Although the studied sample of our previous papers,[5,6] PM6R8-33, manifests a clear antiferroelectric behavior, the new composites show pronounced ferroelectric switching, a phenomenon that needs to be reviewed. We will give the piezoelectric coefficient d_{31}, pyroelectric coefficient γ, and spontaneous polarization P_s for the composites studied herein.

A great advantage of the piezo- and pyroelectric techniques, compared with the standard procedure or the Sawyer–Tower re-polarization current method, is the ability to measure in one case the d_{31} or d_{33} piezoelectric coefficients, which depend on geometric considerations (for determining d_{33} see for example Yablonskii et al.[9]), and in the other case the static value of spontaneous polarization P_s. These techniques allow us to reduce considerably the influence of the conductivity effect in samples, whereas the re-polarization current method results in measurements that are difficult to carry out. All sample mixtures possessed high viscosity and conductivity, and for this reason we could not apply the routine re-polarization current method.

As has been shown in detail,[10] the piezoelectric coefficient d_{31}, in the glassy state, can be calculated from the experimentally available piezoelectric voltage U_{piezo} by the formula $d_{31} = U_{piezo}C/(4LR\Delta p)$, where C (73 pF) is the capacitance of the cell and cables, R (2.7 mm) is the radius of the disk-shaped polymer sample, Δp (12.800 Pa) is the pressure difference and L (0.65d) is the penetration length of the deformation, which is dependent on the thickness of the sample d (110 μm) and the Poisson ratio σ (0.34). The results for PM6R12–M4R8 are plotted in Figure 1. Here, one can observe the temperature dependence of d_{31} on heating of the composite, which was previously poled on cooling, with different direct current (DC) bias voltages. Strong field nonlinearity was confirmed

[*] Prof. E. A. Soto-Bustamante, R. O. Vergara-Toloza
Facultad de Ciencias Químicas y Farmacéuticas
Universidad de Chile
Olivos 1007, 8380492 Santiago (Chile)
E-mail: esoto@ciq.uchile.cl
Prof. S. V. Yablonskii
Institute of Crystallography, Russian Academy of Sciences
Leninsky prosp. 59, 117333 Moscow (Russia)
Prof. W. Haase
Institut für Physikalische Chemie, Technische Universität Darmstadt
Petersenstr. 20, D-64287 Darmstadt (Germany)

[**] S. V. Yablonskii thanks FONDECYT 7000845 and RFBI 03-02.17288 for financial support. E. A. Soto-Bustamante and W. Haase are grateful to Volkswagen Stiftung, VW I/77005 and FONDECYT 1000845 and to Prof. P. Navarrete-Encina for helpful discussions.

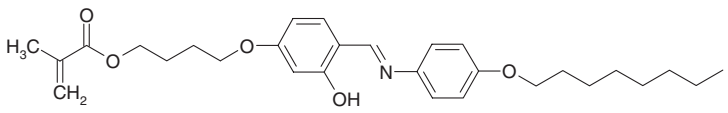

Scheme 1. Chemical formula of the monomer M4R8.

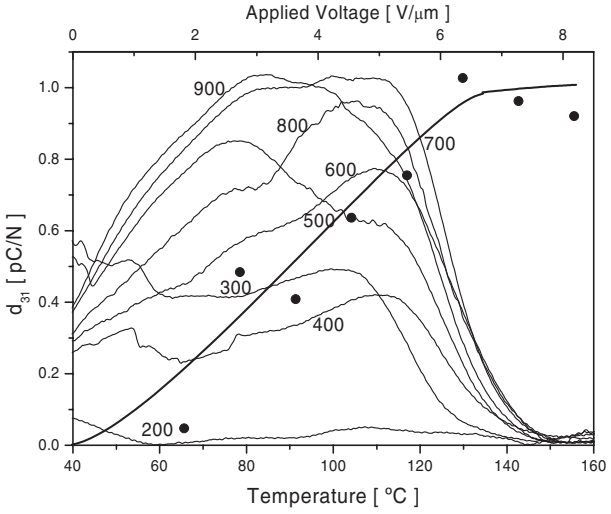

Figure 1. Piezoelectric curves at different DC-bias applied voltage and corresponding electric-field dependence of d_{31} at 105 °C for the PM6R12–M4R8 2:1 composite.

for this composite by plotting the corresponding d_{31} piezoelectric coefficient at 105 °C (Fig. 1, solid circles). The d_{31} coefficient increased with increasing poling voltage, and became saturated at 7 V μm^{-1}, reaching a maximum value of 1.0 pC N^{-1}.

Figure 2 shows the pyroelectric coefficient γ and the macroscopic polarization P_s as function of temperature for the PM6R12–M4R8 composite. The measurements were carried out on cooling under a DC bias field of $E = 10$ V μm^{-1}, which corresponds to the saturation voltage. It is important to note that, as well as in the case of antiferroelectrics mixtures,[5,6] the pyroelectric signal is negligible when individual components are taken separately. On transition from the clearing point to the bilayer smectic C2 phase, γ increased from

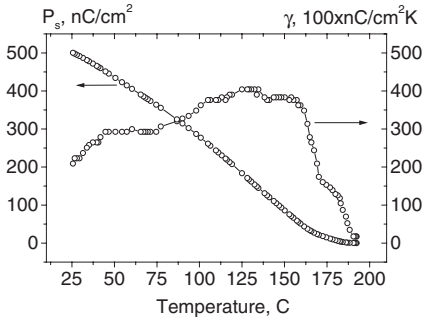

Figure 2. Temperature dependence of the pyroelectric coefficient and the macroscopic polarization of the PM6R12–M4R8 composite.

0.02 nC cm^{-2} K to 4 nC cm^{-2} K. The small signal response in the isotropic phase might be understood as being induced by the electric-field- and temperature-dependent polarization effect. Each consecutive point on the curve was measured after a ten minute exposure to the corresponding electric field.

Assuming a homogeneous distribution of γ across the thickness of the layer, the temperature dependence of P_s was calculated by integrating the absolute value of γ over temperature, according to Equation 1

$$P_s(T) = \int_{T_c}^{T} \gamma \, dT \qquad (1)$$

where T_c corresponds to the second-order transition from the paraelectric to pyroelectric state. During cooling, P_s continuously grows, reaching a maximum value of 500 nC cm^{-2} at room temperature.

The relative scale of γ was introduced by comparison with a known ferroelectric substance. As the standard, we used a commercial ferroelectric liquid-crystalline mixture CS-1029 (CHISSO Corp.), which is in the smectic C* phase at room temperature. The calculated γ for CS-1029 at 25 °C is 0.48 nC cm^{-2} K, which corresponds to 3 nC cm^{-2} K for PM6R12-M4R5. The pyroelectric signals of the standard and sample were compared at different frequencies. At high frequencies, the penetration depth of the diffusion temperature wave is less than the cell thickness, and practically independent of heat characteristics such as the thermoconductivity and thermocapacity of both the standard and the investigated sample. This was demonstrated when we compared values of γ for the sample and CS-1029 versus frequency: a constant dependence over 10 kHz was observed.

The shape of the hysteresis loop is one of the major criteria for classifying nonlinear dielectrics as ferro-, ferri- or antiferroelectric types. Usually, hysteresis loops are represented in coordinates of electric displacement versus external electric field. However, hysteresis loops in coordinates of γ versus external electric field differ only quantitatively from the former. Indeed, using the definition of the volume polarization $P_s = (N\mu/V)\langle\cos\varphi\rangle$ as well as the pyroelectric coefficient $\gamma = d\mu/dT(N/V)\langle\cos\varphi\rangle$, one can see that the ratio P_s/γ at a given temperature is constant. Here, N is the number of dipoles with the moment μ within the volume V, and $\langle\cos\varphi\rangle$ is the average value of the cosine of the angle between the dipole direction and the net polarization direction.

The experimental curves show a strongly pronounced nonlinear behavior of γ with the applied field (Fig. 3). Hysteresis loops were taken at elevated temperatures, 159.2 °C and 166.9 °C, and demonstrated a ferroelectric-like behavior; possessing non-zero coercive fields with a supralinear growth of the pyroelectric response, and the saturation of the signal at moderate values of the bias voltage.[11]

On the other hand, a curve obtained at 141 °C also behaved in a supralinear fashion. To some extent, however, the ferroelectric character is lost at zero field, producing an asymmetry in the hysteresis loop. This could be understood as evidence

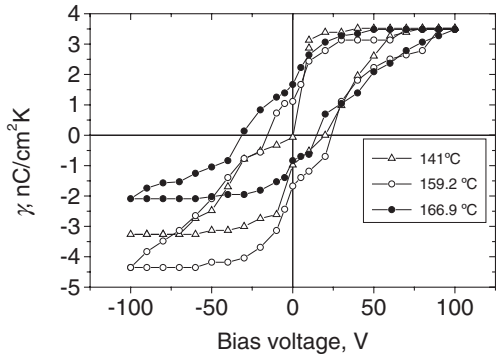

Figure 3. Ferroelectric hysteresis loops in coordinates of the DC-bias-voltage pyroelectric coefficient obtained for PM6R12-M4R8 composite at three different temperatures.

of an antiferroelectric- to ferroelectric-phase transition. It must be emphasized that, in liquid crystals, antiferroelectric phases exist in general at a lower temperature than ferroelectric ones, a situation contrary to that observed in solids.[12] We must also bear in mind that at this temperature the viscosity of the PM6R8–M4R8 composite is high and thus restricts the dipole reversibility movement. This mainly affects the polymeric part of the composite, thus permitting the observed asymmetric behavior.

The ferroelectric hysteresis loop at 110 °C, in the smectic C phase of a slightly different mixture, PM6R12–M4R6 is shown in Figure 4. The lack of the three stable states for this mixture, and its ability to change the sign of the pyroelectric response, which corresponds to a change in the phase angle of 180°

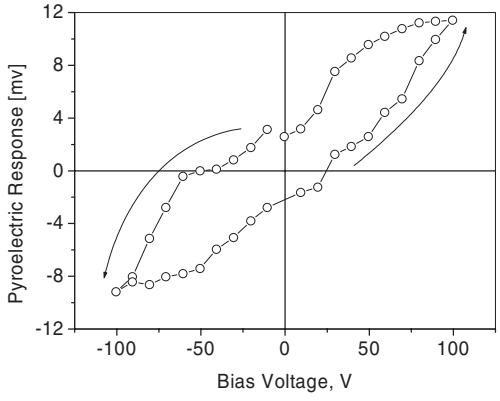

Figure 4. Hysteresis loop for PM6R12-M4R6 composite at 110 °C obtained by the light intensity modulation method. Arrows show the direction of measurements.

achieved by changing the polarity of the applied bias, testifies in favor of the ferroelectric switching. In the glassy state, the pyroelectric response should remain stable with time. Some old samples of PM6R8-33[4–6] stored at room temperature and in atmospheric humidity, and which belong to the same family of compounds, retained their polarization for more than four years.

The structural element of the mesophase in a tilted side-chain polymer is shown in Figure 5a. For simplicity, dissolved monomers are not shown. Three vectors: **n** (normal to the smectic layers), **c** (*c*-director), and **P** (spontaneous polarization) make up a right- or left-handed coordinate system, which reflects the chiral character of the mesophase due to the spontaneous symmetry breakdown.[13]

We should emphasize that the intrinsic nature of the achiral phases and their stability is still an open question. Regarding this point, and according to our observations, we conclude that polymer–monomer mixtures with shorter monomer molecules promote the ferroelectric state. This evidence is in accordance with the simplified picture illustrating the stability of a synclinic state.[14] In the case of the smectic C2 phase, partial permeation of molecules from one layer to another may take place. Such fluctuations are permitted in a synclinic ordered system, as shown in Figures 5b,c. Therefore, it is obvious to assume that they may be facilitated in the case of small molecules.

In a ferroelectric arrangement, a synclinic order in the mesogenic interface is allowed, whereas for antiferroelectricity, an anticlinic order can be assumed. Obviously the anticlinic arrangements, shown in Figures 5d,e, give rise to a decrease in the system entropy that can be compensated by a decrease of electrical energy in the antiferroelectric state.

A basic characteristic of pyroelectric materials, for practical applications, is the so-called "figure of merit", which is defined as the ratio of the pyroelectric coefficient to the effective dielectric permittivity. The variable voltage U_p generated by a pyroelectric sensor is proportional to the pyroelectric voltage $U_p \approx \Delta q/C \approx \gamma_s/\varepsilon$. Here Δq corresponds to the increment of charges in the electrode surface due to the inherent capacitance promoted by the pyroelectric effect, and C is the capacitance of the cell. The best of our samples have a "figure of merit" in the glassy state equal to 0.75, comparable to single crystal triglycine sulfate (TGS) which is used for pyroelectric detectors.[15]

We have demonstrated sufficient evidence of ferroelectric behavior in mixtures composed of an achiral liquid crystalline side-chain polymer (PM6R12) and an achiral liquid crystalline monomer (either M4R5, M4R6, or M4R8). The mixtures manifested high pyroelectric activity, with values of spontaneous polarization close to the theoretical limit and a "figure of merit" in one of the studied cases comparable to the value of the classic organic ferroelectric TGS.

Experimental

The compounds were synthesized using a convergent synthetic pathway previously described [16,17]. Characterization was carried out using ^{1}H NMR spectroscopy (300 MHz spectrometer Bruker, WM 300), infrared spectroscopy (FTIR Paragon Spectrometer, 100PC), and elemental analysis (Perkin Elmer, 240 B). A detailed chemical description of the monomer M4R5 has been already published [18], therefore the remaining monomeric compounds, i.e., M4R6 and M4R8 will not be described further. A chemical description of poly[2-methyl-2-propenoic acid 4-[3-hydroxy-4–[[[6-dodecyloxy) phenyl] imino]-methyl] phenoxy] hexyl ester], PM6R12, is as follows.

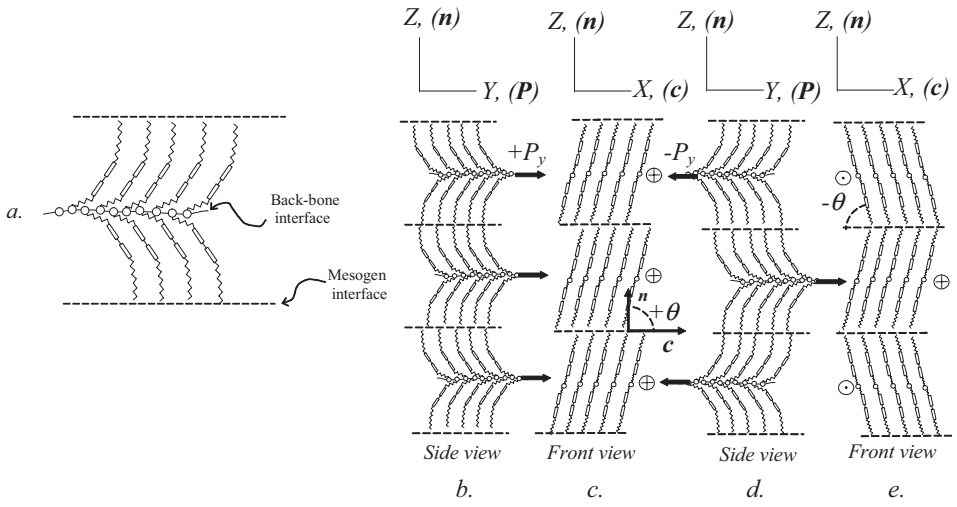

Figure 5. a) Structural element of the mesophase composed of polymer molecules in ferroelectric (b,c) and antiferroelectric (d,e) arrangements.

PM6R12: ^{1}H NMR ($CDCl_3$) δ [ppm]: 13.76 (s, 1H, Ph–O*H*); 8.26 (s, 1H, Ph–C*H*=N); 7.03 (m, 3H, Ph–*H*); 6.73 (m, 2H, Ph–*H*); 6.31 (m, 2H, Ph–*H*); 3.76 (m, 6H, CH_2–O_2C, CH_2–OPh); 1.65–1.18 (m, 28H, –CH_2–CH_2–CH_2–CH_2–; CH_3–C–C_3); 0.80 (t, 3H, –CH_2–CH_3).

IR (KBr) ν [cm^{-1}]: 1728s (C=O), 1618s (C=N), 1296s, 1251s, 1190s, 1168w, 1139m, 1115m (C–O), 648m, 588m, 534s, 465m.

Anal. calcd. for $(C_{35}H_{51}NO_5)_n$; (M = 565.70)$_n$: C, 74.30; H, 9.09; N, 2.48. Found: C, 74.07; H, 9.18; N, 2.68

Monomers show the simultaneous occurrence of monolayered smectic A and C phases. Short monomers, such as M4R5, also developed a nematic phase before the isotropic state [18]. In polymers, bilayered smectic C2 phases were detected [19,20]. The phase-transition temperature and corresponding enthalpies are summarized in Table 1. They were determined using a differential thermal analyzer (Mettler Toledo FP84HT-FP 90, accuracy ±0.1 K). The data for PM6R12 and

Table 1. Phase transition temperature and enthalpy by heating for PM6R12, monomers, and the investigated composites.

Sample	Mesophase	Enthalpy [J/g] [a]
M4R5 [18]	C–41.4–S_C–66.4–S_A–83.8–N–87.1–I	45.00–n/d–2.50–1.54
M4R6 [18]	C–30.3–S_C–58.7–S_A–87.8–I	45.66–n/d–5.12
M4R8 [18]	C–38.3–S_C–70.4–S_A–92.5–I	50.26–n/d–6.83
PM6R12 [19]	g–n/d–S_{C2}–190.5–I	21.2
PM6R12-M4R5	g–100.5–S_{C2}–155.6–I	n/d
PM6R12-M4R6	g–92.8–S_{C2}–162.6–I	15.7
PM6R12-M4R8	g–93.2–S_{C2}–163.5–I	13.5
CS-1029	C–(–)18.0–S_{C*}–73.0–S_A–85.0–N*–95.0–I	n/d

[a] n/d: not determined.

the standard material CS-1029 used for calibrations are also included. A detailed description of DTA traces and X-ray diffraction characterization for the new composites will be presented separately.

The average molecular weight $\overline{M}_w$ of PM6R12 is 108.100, which corresponds to a degree of polymerization *Pw* of 191, with a polydispersity index *DI* of 2.609 [19].

The piezoelectric setup for measuring the apparent low-frequency piezoelectric longitudinal modulus d_{31} has been described previously [10]. The sample was mounted in a cavity and a low-frequency pressure was applied by a loudspeaker at the end of a pipe connected to the cavity, exciting an acoustical wave with a pressure amplitude Δp at the sample location. The piezoelectric response was detected by a lock-in amplifier (EG&G Model 5460) in voltage-sensitive mode. Cells consisting of two indium tin oxide (ITO)-covered glass slides separated by a spacer of 110 μm thickness were filled with the composites at slightly above the clearing temperature.

The pyroelectric setup used in the measurements has been described previously [21]. Temperature variations of the samples were caused by a modulated light from a semiconductor laser (λ = 690 nm, P = 27 mW, modulation capability from DC to 5 MHz). A modulation frequency of 70 Hz was provided from a function generator (HP 33120A, ranging from 0.1 mHz to 15 MHz). The sample was connected to a lock-in amplifier (EG&G Model 5460) operating in the voltage-sensitive mode. The composites were confined in commercial EHC cells 10 μm thick by capillarity at a temperature slightly above the clearing point.

For both piezo- and pyroelectric experiments, the cells were placed on a temperature-controllable hot stage and the composites were poled down to room temperature under a DC electric field. The measurements were carried out by heating to the isotropic state without a field.

By measuring the intrinsic electrical properties of our materials, such as γ, we can estimate the spontaneous polarization P_s. The pyroelectric hysteresis loops that characterize the antiferro- or ferroelectric nature of the composites were determined with the pulse pyroelectric technique [22] based on the light-intensity modulation method [23]. The curves in Figure 4 were obtained using a YAG laser (λ = 1.06 μm, E = 4 mJ, τ = 100 μs), in a 10 μm thick EHC cell, with ITO electrodes, and covered with polyimide layers. The capacitance and resistance of the cell at room temperature were C = 50 pF and $R \gg 20$ MΩ, respectively.

[1] R. B. Meyer, L. Liebert, L. Strzelecki, P. Keller, *J. Phys.* **1975**, *36*, L-69.

[2] S. A. Pikin, *Structural Transformations in Liquid Crystals*, Gordon and Breach, New York **1991**.

[3] *Ferroelectric Liquid Crystals, Principles, Properties & Applications* (Eds: R. Blinc, J. W. Goodby), Gordon and Breach, New York **1991**.

[4] E. A. Soto-Bustamante, S. V. Yablonskii, L. A. Beresnev, L. M. Blinov, W. Haase, W. Dultz, Y. G. Galyametdinov, *German Patent DE 195 47 934*, **1997**.

[5] E. A. Soto-Bustamante, S. V. Yablonskii, B. I. Ostrovskii, L. A. Beresnev, L. V. Blinov, W. Haase, *Chem. Phys. Lett.* **1996**, *260*, 447.

[6] E. A. Soto-Bustamante, S. V. Yablonskii, B. I. Ostrovskii, L. A. Beresnev, L. V. Blinov, W. Haase, *Liq. Cryst.* **1996**, *21*, 829.
[7] T. Niori, T. Sekine, J. Watanabe, T. Furukawa, H. Takezoe, *J. Mater. Chem.* **1996**, *6*, 1231.
[8] F. Tournilhac, L. M. Blinov, J. Simon, S. V. Yablonskii, *Nature* **1992**, *359*, 621.
[9] S. V. Yablonskii, S. Grossmann, T. Weyrauch, R. Werner, E. Soto-Bustamante, W. Haase, S. G. Yudin, L. M. Blinov, *Ferroelectrics* **2000**, *247*, 343.
[10] S. V. Yablonskii, E. I. Kats, M. V. Kozlovskii, T. Weyrauch, E. A. Soto-Bustamante, D. B. Subachius, W. Haase, *Mol. Mater.* **1994**, *3*, 311.
[11] M. E. Lines, A. M. Glass, *Principles and Applications of Ferroelectrics and Related Materials*, Clarendon Press, Oxford, UK **1977**, Ch. 4.
[12] S. T. Lagerwall, *Ferroelectric and Antiferroelectric Liquid Crystals*, Wiley-VCH, Weinheim, Germany **1999**, Ch. 13.
[13] D. R. Link, G. Natale, R. Shao, J. E. MacLennan, N. A. Clark, E. Korblova, D. M. Walba, *Science* **1997**, *278*, 1924.
[14] D. R. Link, N. A. Clark, B. I. Ostrovskii, E. A. Soto-Bustamante, *Phys. Rev. E* **2000**, *61*, 37.
[15] E. Yamaka, in *The applications of ferroelectric polymers*, (Eds: T. T. Wang, J. M. Herbert, A. M. Glass), Chapman and Hall, New York **1988**, Ch. 14.
[16] E. A. Soto-Bustamante, Y. G. Galyametdinov, K. Griesar, E. Schuhmacher, W. Haase, *Macromol. Chem. Phys.* **1998**, *199*, 1337.
[17] E. A. Soto-Bustamante, W. Haase, *Liq. Cryst.* **1997**, *23*, 603.
[18] E. A. Soto-Bustamante, D. Saldaño-Hurtado, R. O. Vergara-Toloza, P. A. Navarrete-Encina, M. A. Athanassopoulou, *Liq. Cryst.* **2003**, *30*, 17.
[19] R. Werner, E. A. Soto-Bustamante, P. A. Navarrete-Encina, W. Haase, *Liq. Cryst.* **2002**, *29*, 713.
[20] E. A. Soto-Bustamante, R. Vergara-Toloza, D. Saldaño-Hurtado, P. A. Navarrete-Encina, *Liq. Cryst.* **2003**, *30*, 585.
[21] E. A. Soto-Bustamante, P. A. Navarrete-Encina, T. Weyrauch, R. Werner, *Ferroelectrics* **2000**, *243*, 125.
[22] L. A. Beresnev, L. M. Blinov, *Ferroelectrics* **1981**, *33*, 129.
[23] S. B. Lang, *Ferroelectrics* **1991**, *118*, 343.